Environmental Science and Pollution Research (2022) 29:17866–17877
https://doi.org/10.1007/s11356-021-17089-y

RESEARCH ARTICLE

Electrochemically activated peroxymonosulfate for the abatement of chloramphenicol in water: performance and mechanism

Yu-Qiong Gao[1] · Jin-Qiang Zhou[1] · Han Ning[1] · Yan-Yan Rao[1] · Nai-Yun Gao[2]

Received: 23 May 2021 / Accepted: 13 October 2021 / Published online: 21 October 2021

Abstract

In this study, electrochemically activated peroxymonosulfate (EC/PMS) with a sacrificial iron electrode was used for the removal of chloramphenicol (CAP) from water. Compared to electrolysis alone, peroxymonosulfate (PMS) alone, and Fe^{2+}/PMS, EC/PMS significantly enhanced the CAP degradation. Various parameters, such as the applied current, electrolyte concentration, and PMS dose, were investigated to optimize the process. In addition, acidic conditions facilitated the CAP degradation. The presence of Cl^- slightly enhanced the CAP degradation, while both HCO_3^- and NO_3^- exhibited an inhibitory effect on the CAP degradation. The floccules were also analyzed after the reaction by XPS and XRD. Quenching experiments indicated that both sulfate radicals ($SO_4^{\bullet-}$) and hydroxyl radicals (•OH) were responsible for the CAP degradation. In addition, the degradation products were identified by LC/TOF/MS, and the degradation pathways were proposed accordingly. These results indicated that EC/PMS is a promising treatment process for the remediation of water polluted by CAP.

Keywords Chloramphenicol · Electrochemistry · Peroxymonosulfate · Sulfate radical · Influencing factor · Mechanism

Introduction

Various kinds of antibiotics have been produced and applied worldwide for the treatment of human and animal diseases caused by microbial infectious diseases. As a result, a large amount of antibiotics has been discharged into the environment via effluent from hospitals and wastewater treatment plants (WWTPs), pharmaceutical industry wastewater release, improper discharge of treated landfill leachate, etc. (Kümmerer 2009). Residual antibiotics in the water environment pose potential risks to aquatic organisms as well as to human health, and they can also cause the formation of antibiotic-resistant bacteria (ARB) and antibiotic resistance genes (ARG) (Danner et al. 2019; Kovalakova et al. 2020). Due to excessive consumption and incorrect treatment methods, antibiotic pollution in the water environment has raised widespread concern and become a common environmental problem (Yan et al. 2015). As one of the commonly used antibiotics, chloramphenicol (CAP) is a broad-spectrum antibiotic for both humans and animals owing to its high activity against many gram-positive and gram-negative bacteria (Wu et al. 2017). It has been reported that a considerable proportion of CAP is directly excreted in the aquatic environment via urine or feces after its intake by humans or animals (Zhou et al. 2017). Moreover, many antibiotics, including CAP, are stable in water and are resistant to traditional wastewater treatment owing to their physical and chemical properties (Cao et al. 2020; Zhou et al. 2009). Accordingly, nano- to micrograms CAP has been frequently detected in aquatic environments. In Germany, CAP concentration was up to 0.56 μg/L and 60 ng/L, as detected in the effluent of one WWTP and in surface water, respectively (Hirsch et al. 1999). As detected in the Pearl River of China, the concentration of CAP was as high as 266 ng/L and 187 ng/L in the high and low water seasons, respectively (Xu et al. 2007). Therefore, effective techniques are urgently needed for efficient CAP removal.

Many techniques have been extensively adopted for eliminating CAP from water, such as adsorption (Fan et al.

Responsible Editor: Ricardo A. Torres-Palma

✉ Yu-Qiong Gao
gaoyq@usst.edu.cn

[1] School of Environment and Architecture, University of Shanghai for Science and Technology, Shanghai 200093, China

[2] State Key Laboratory of Pollution Control and Resource Reuse, College of Environmental Science and Engineering, Tongji University, Shanghai 200092, China

2010), ferrate (Zhang et al. 2021), and solar photoelectro-Fenton (Garcia-Segura et al. 2014). Among these techniques, advanced oxidation processes (AOPs) are promising methods for destruction of many organic contaminants in water, which are based on the generation of highly oxidizing hydroxyl radicals (•OH). Recently, sulfate radical ($SO_4^{\bullet-}$)–based advanced oxidation processes (SR-AOPs) have attracted much interest recently due to their excellent performance in degrading various refractory organic contaminants from water (Oh et al. 2016). In SR-AOPs, organic contaminants can be decomposed to CO_2 and H_2O as a result of $SO_4^{\bullet-}$, which has a strong oxidation ability (E_0 = 2.5~3.1 V), high pH adaptability (2~10), and a long lifetime (30~40 μs) (Qi et al. 2017). Generally, $SO_4^{\bullet-}$ can be generated mainly via heat, UV irradiation, and transition metal activation of persulfate (PS) and peroxymonosulfate (PMS). PMS is considered to be a green oxidant that is easily activated for a variety of industrial and consumer applications involving disinfection (Tan et al. 2018). The oxidation ability of PMS at room temperature is low (E_0 = 1.82 V) (Wang and Chu 2012), but it can still be activated by various methods to produce $SO_4^{\bullet-}$. Over the past few years, ferrous-activated PMS (Fe^{2+}/PMS) has been adopted as an effective tool for $SO_4^{\bullet-}$ production for the removal of organic contaminants. Owing to its low cost, nontoxicity, and high activity, Fe^{2+} is always selected as an ideal activator of PMS or PS (Huang et al. 2021; Zou et al. 2013). Furthermore, owing to its asymmetrical structure (HO-O-SO_3^-) and lower bond dissociation energy, PMS is considered to be more readily activated by Fe^{2+} than PS (Oh et al. 2016).

However, like the Fenton reaction, the Fe^{2+}/PMS process contains the disadvantage of a narrow acidic pH range because Fe^{2+} tends to transform into iron hydroxides at neutral or alkaline pH; this conversion may hinder the transformation of Fe^{3+} to Fe^{2+} (Song et al. 2020). Furthermore, the weak reversibility of the transformation of Fe^{3+} to Fe^{2+} reduces the activation efficiency of PMS and the utilization of Fe^{2+}; therefore, a higher dose of ferrous salt is needed to continuously activate PMS, which may also quench $SO_4^{\bullet-}$ and produce a large amount of iron sludge (Ali et al. 2020). An effective approach to address such drawbacks is introducing an electric field into the Fe^{2+}/PMS system (Brillas et al. 2009). Electrochemically activated PMS (EC/PMS) that uses Fe as the sacrificial anode is an ideal alternative for PMS activation because it can overcome the drawback of the slow Fe^{3+}/Fe^{2+} cycle that occurs in the Fe^{2+}/PMS process (Govindan et al. 2014). The EC/PMS process is a combination of electrochemical and Fe^{2+}/PMS processes. In the EC/PMS system, soluble Fe^{2+} is continuously released to the solution from the surface of the iron electrode through anodic oxidation. Meanwhile, the reduction of Fe^{3+} occurs at the cathode (Wang and Chu 2011). Compared with the Fe^{2+}/PMS process, EC/PMS can not only control the release of Fe^{2+} by adjusting the applied current but also accelerate the Fe^{3+}/Fe^{2+} cycle, thus overcoming the low activation efficiency of PMS and the iron sludge problem caused by addition of excessive Fe^{2+} in the Fe^{2+}/PMS process. In addition, electrolysis can also directly activate PMS to generate $SO_4^{\bullet-}$ (Wang and Chu 2011).

Herein, an electrochemically activated PMS (EC/PMS) process that uses iron as the sacrificial anode was proposed for the abatement of CAP. Several influencing factors, including the applied current, electrolyte concentration, PMS dose, initial solution pH, and common anions, were investigated to determine their effect on the CAP degradation performance. Moreover, the floccules formed during the reaction were characterized by X-ray photoelectron spectroscopy (XPS) and X-ray diffraction (XRD). The radical species responsible for CAP degradation were investigated by quenching experiments. In addition, the major degradation products of CAP were identified by LC/TOF/MS, and the degradation pathways of CAP during the EC/PMS process were proposed.

Materials and methods

Materials

Chloramphenicol (CAP, ≥98%) was purchased from Sigma-Aldrich (St. Louis, MO, USA). Peroxymonosulfate ($KHSO_5 \cdot 1/2KHSO_4 \cdot 1/2K_2SO_4$, ≥47%) was purchased from Aladdin Chemistry Co., Ltd. (Shanghai, China). Anhydrous sodium sulfate (Na_2SO_4, ≥99%) was purchased from Sinopharm Chemical Reagent Co., Ltd. (Shanghai, China). Chromatographic reagent grade acetonitrile used as the mobile phase was purchased from J. T. Baker (USA). All other chemicals used in the study were of at least analytical grade. Milli-Q water (18.2•MΩ cm) was used to prepare all the experimental solutions.

Experimental procedure

The experiments were carried out in a 250-mL undivided single-compartment glass cell by using a plate iron anode (2 cm × 4 cm) and a plate cathode (stainless steel) of the same dimensions (Fig. 1). Constant current electrolysis conditions were maintained by a DC-regulated power supply provided by Dongguan Tongmen Electronic Technology Co., Ltd. (China). The two electrode plates were fixed parallel to each other at a distance of 2.5 cm. The reaction temperature was kept at 20 ± 1 °C by immersing the reaction cell in a water bath. In a typical run, a mixed solution of CAP and electrolyte (Na_2SO_4) was added to the reactor and then

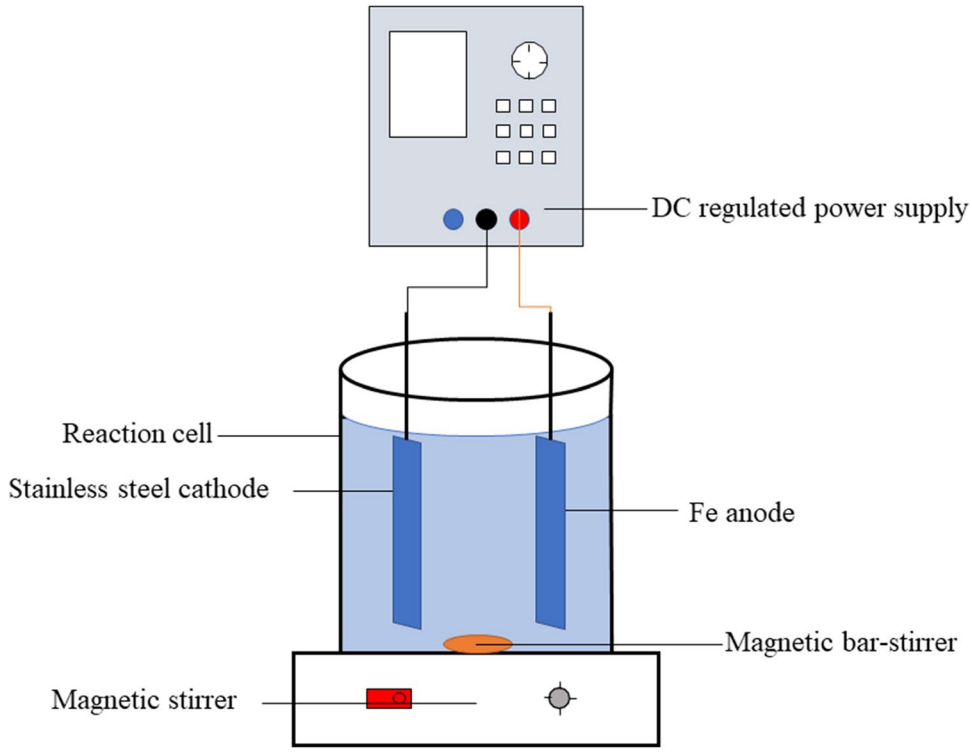

Fig 1 Scheme of the experimental equipment

stirred by a magnetic stirrer. After adding a certain dose of PMS into the reaction solution and turning on the DC power, the reaction was initiated. The initial solution pH was adjusted by H_2SO_4 or NaOH. At predetermined time intervals, the samples were withdrawn from the electrolytic cell and filtered through 0.45-μm membranes and then quenched with prefilled methanol immediately before analysis.

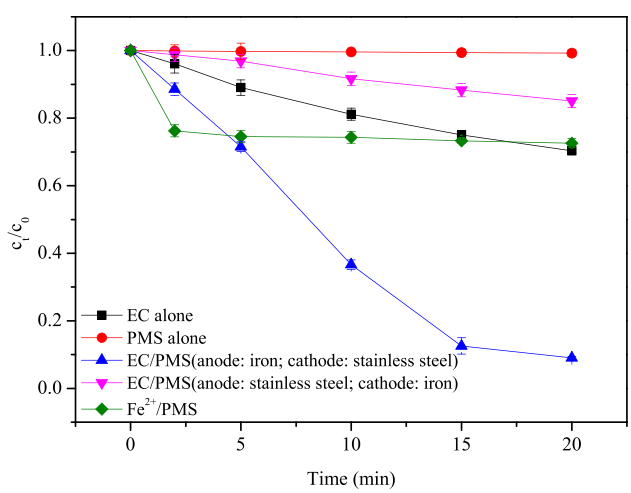

Fig. 2 CAP degradation under different systems. Experimental conditions: $[CAP]_0$ = 10 μM, $[PMS]_0$ = 0.5 mM, $[Fe^{2+}]_0$ = 621 μM, current = 25 mA, $[Na_2SO_4]_0$ = 25 mM, pH_0 = 7

Analysis

The concentration of CAP was determined by Shimadzu HPLC consisting of an LC-20AB pump and an SPD-20A UV detector set at 275 nm. A mixture of acetonitrile/water (60:40, v/v) was used as the mobile phase, and the flow rate was set at 0.8 mL/min. The concentration of PMS was determined by UV spectrophotometry according to the method described by Wacławek et al. (2015). The floccules were characterized by XRD (Rigaku Ultima IV) and XPS (Thermo Scientific K-Alpha) after the reaction. The CAP degradation products were analyzed using ultra-performance liquid chromatography and quadrupole time-of-flight mass spectrometry (Agilent 1290 UPLC/6550 Q-TOF) with a Waters BEH C18 column (2.1 × 100 mm, 1.7 μm). An elution gradient with two mobile phases, MQ water (A) and acetonitrile (B), was programmed as follows (min, %A): (0, 90), (1, 90), (8, 10), (12, 10), (12.1, 90), and (13, 90). The flow rate was 0.3 mL/min. The mass spectrometer was operated in negative ionization mode using an electrospray ionization (ESI) source. The spray voltage, sheath gas temperature, and sheath gas flow were set at −3200 V, 350°C, and 12 L/min, respectively. Full scan mode was set to m/z 50–500.

Results and discussion

Comparative study of different systems

We first investigated CAP degradation in five different systems: (1) EC alone, (2) PMS alone, (3) EC/PMS process, (4) EC/PMS process using stainless steel as the anode and iron as the cathode, and (5) Fe^{2+}/PMS. As shown in Fig. 2, no obvious removal was observed when CAP was treated by PMS oxidation alone because PMS is stable at ambient temperature and its redox potential is very limited (E^0 = 1.82 V) (Wang and Chu 2012). EC alone achieved 29.7% CAP removal, implying that the coagulation mechanism plays a role in CAP removal. As expected, approximately 91.0% CAP removal was achieved within 20 min in the EC/PMS system using iron as the anode and stainless steel as the cathode. During the EC/PMS process, Fe^{2+} was first electrochemically produced from the sacrificial iron anode, which could serve as the activator of PMS to generate sulfate radicals ($SO_4^{\bullet-}$) (Eqs. (1) and (2)), which accelerate CAP degradation. Fe^{2+} was regenerated on the cathode plate according to Eq. (3), maintaining a relatively proper level of Fe^{2+} in the system. In addition, after swapping the two electrode plates (i.e., using stainless steel as the anode and iron as the cathode), we also noticed that 14.9% removal of CAP was achieved within 20 min, which indicated that electrolysis can also directly activate PMS to form $SO_4^{\bullet-}$ and/or •OH (Eqs. (4) and (5)) (Wang and Chu 2011). We should also notice that direct oxidation of CAP on anode is also expected to occur.

$$Fe \rightarrow Fe^{2+} + 2e^{-}(Anode) \tag{1}$$

$$Fe^{2+} + HSO_5^{-} \rightarrow Fe^{3+} + SO_4^{\bullet-} + OH^{-} \tag{2}$$

$$Fe^{3+} + e^{-} \rightarrow Fe^{2+}(Cathode) \tag{3}$$

$$HSO_5^{-} + e^{-} \rightarrow SO_4^{\bullet-} + OH^{-} \tag{4}$$

$$HSO_5^{-} + e^{-} \rightarrow SO_4^{2-} + \cdot OH \tag{5}$$

A comparison between the EC/PMS system and the ferrous ion–activated PMS (Fe^{2+}/PMS) system was also conducted. The concentration of added Fe^{2+} in the EC/PMS system was calculated through Faraday's law (Eq. (6)) with a reaction time of 20 min.

$$C = \frac{I \times t}{F \times Z \times V} \tag{6}$$

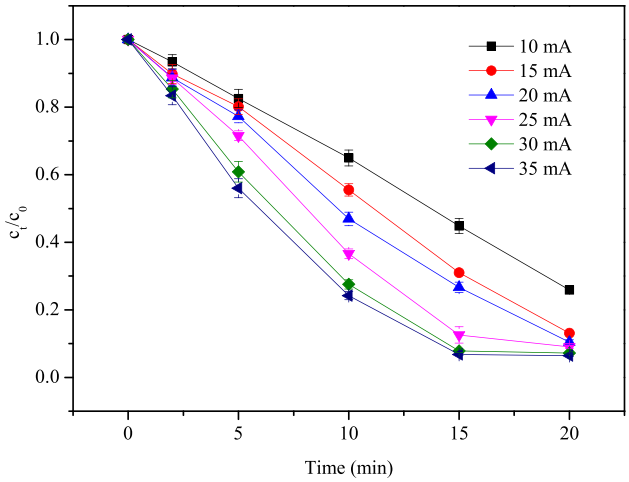

Fig. 3 Effect of applied current on CAP degradation. Experimental conditions: $[CAP]_0$ = 10 μM, $[PMS]_0$ = 0.5 mM, $[Na_2SO_4]_0$ = 25 mM, pH_0 = 7

where C is the molecular concentration of Fe^{2+} generated in the system (mol/L), Z is the number of electrons (2 equivalents/mol), F is Faraday's constant (96,485.3 Coulombs/mol), I is the given current (A), t is the reaction time (s), and V is the volume of electrolyte (L).

As seen, the degradation behavior of CAP in the Fe^{2+}/PMS system exhibited a fast and then a slow stage along with the reaction time. The fast stage was attributed to the relatively higher initial Fe^{2+} concentration, and the slower stage was caused by the depletion of Fe^{2+} and inadequate regeneration of Fe^{3+} to Fe^{2+}, which inhibited the generation of $SO_4^{\bullet-}$ (Tan et al. 2018). We also noticed that the final removal efficiency of CAP by the EC/PMS system was higher than that of the Fe^{2+}/PMS system. This phenomenon could be ascribed to the different levels of Fe^{2+} use in the two systems. In the Fe^{2+}/PMS system, excess Fe^{2+} competed with CAP for the generated $SO_4^{\bullet-}$ as well as rapidly consumed PMS in the initial stage and thus hindered the CAP degradation in the following stage (Eq. (7)) (Rastogi et al. 2009). However, in the EC/PMS system, Fe^{2+} was gradually released from the iron electrode, and Fe^{2+} could also be regenerated via cathodic reduction of Fe^{3+}, which maintained CAP degradation over time.

$$Fe^{2+} + SO_4^{\bullet-} \rightarrow Fe^{3+} + SO_4^{2-} \tag{7}$$

Effect of applied current

The effect of the applied current on CAP degradation by the EC/PMS system is shown in Fig. 3. As the applied current increased from 10 to 25 mA, the removal rate of CAP increased from 74.1 to 91.0% within 20 min. As the

applied current further increased to 35 mA, the removal rate of CAP slightly increased from 91.0 to 93.5%. Increasing the applied current density led to more rapid Fe^{2+} production, which improved the decomposition of PMS to generate more $SO_4^{\bullet-}$, thus enhancing CAP degradation. In addition, a higher applied current also led to a faster generation of $SO_4^{\bullet-}$ via an electron transfer reaction. Additionally, more Fe^{2+} was also generated at a higher applied current; thus, the excess Fe^{2+} may have acted as a $SO_4^{\bullet-}$ scavenger and compete with CAP for $SO_4^{\bullet-}$ (Eq. (7)) (Rastogi et al. 2009).

Effect of electrolyte concentration

The effect of electrolyte concentration (Na_2SO_4) on CAP degradation by the EC/PMS system is shown in Fig. 4. As the Na_2SO_4 concentration increased from 5 to 25 mM, the removal rate of CAP also increased from 81.5 to 91.0%. The electrical conductivity of the solution was directly influenced by the electrolyte concentration, and increasing the Na_2SO_4 concentration increased the conductivity of the reaction solution, resulting in a lower energy loss during the drop in ohmic resistance of the solution (Periyasamy and Muthuchamy 2018).

Effect of PMS dose

The effect of PMS dose on CAP degradation is shown in Fig. 5a. The removal rate increased from 56.3 to 91.0% as the PMS dose increased from 0.1 to 0.5 mM, and then the removal rate of CAP decreased to 77.1% as the PMS concentration further increased to 1 mM. The increment of CAP removal rate when PMS concentration increased from 0.1 to 0.5 mM is ascribed to the fact that PMS served as the source of $SO_4^{\bullet-}$ in the EC/PMS system; thus, more reactive species were produced to degrade CAP at higher PMS concentrations. However, if the PMS concentration was too high, side reactions occurred (Eqs. (8) and (9)), leading to the self-quenching of $SO_4^{\bullet-}$ and/or •OH by excessive PMS (Shukla et al. 2010).

It is of interest to observe that the initial degradation rate of CAP (computed as $\Delta c/\Delta t$ over the first 2 min, μM/min) was decreased from 1.64 to 0.33 μM/min with the increment of PMS from 0.1 to 1 mM. This observation can also be explained by the unfavorable consumption of $SO_4^{\bullet-}$ and •OH according to Eqs. (8) and (9), leading to the production of the less reactive $SO_5^{\bullet-}$ and thus slowing the CAP degradation. However, the overall removal of CAP at the end of the process was still observed at a relatively higher PMS concentration because the PMS, which served as the $SO_4^{\bullet-}$ source, was completely consumed at a relatively lower PMS concentration during the 20-min reaction (Fig. 5b).

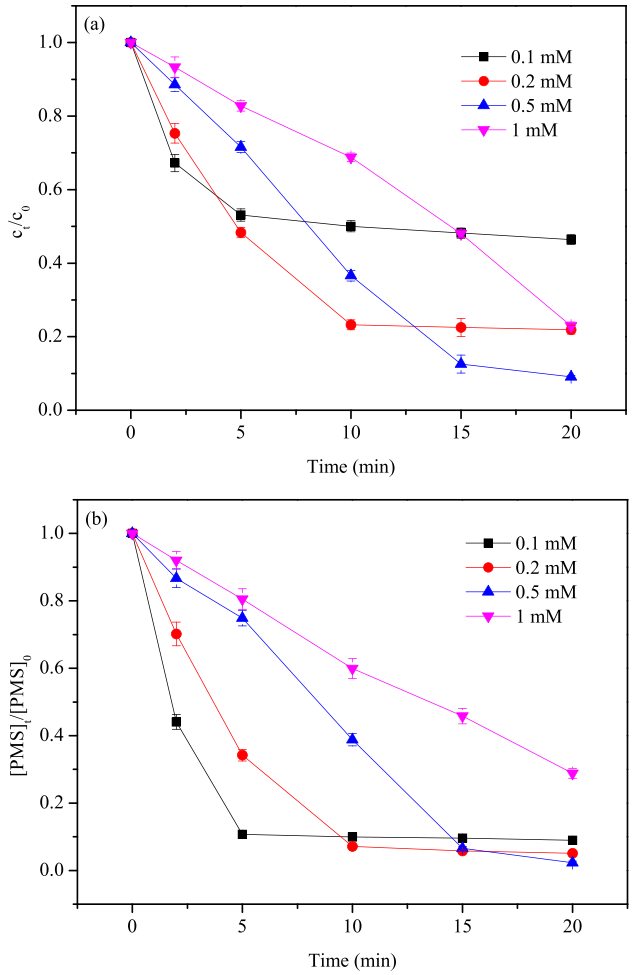

Fig. 5 **a** Effect of PMS dose on CAP degradation; **b** change in $[PMS]_t/[PMS]_0$ during the reaction. Experimental conditions: $[CAP]_0$ = 10 μM, current = 25 mA, $[Na_2SO_4]_0$ = 25 mM, pH_0 = 7

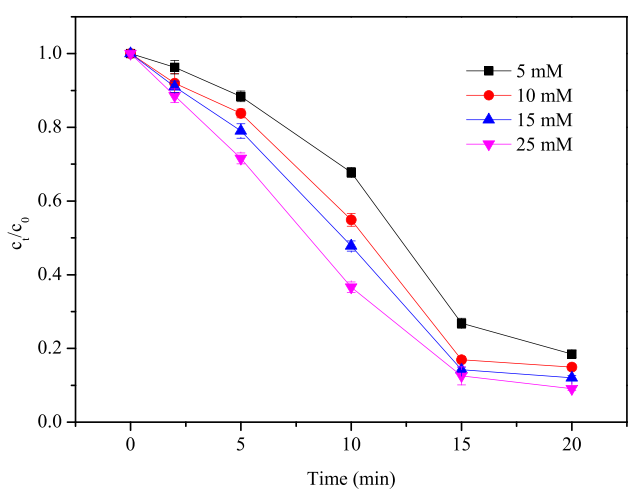

Fig. 4 Effect of electrolyte concentration on CAP degradation. Experimental conditions: $[CAP]_0$ = 10 μM, $[PMS]_0$ = 0.5 mM, current = 25 mA, pH_0 = 7

$$SO_4^{\bullet-} + HSO_5^- \rightarrow HSO_4^- + SO_5^{\bullet-} k < 10^5 M^{-1} s^{-1} \quad (8)$$

$$\cdot OH + HSO_5^- \rightarrow H_2O + SO_5^{\bullet-} k = 1.7 \times 10^7 M^{-1} s^{-1} \quad (9)$$

Effect of initial solution pH

The effect of the initial solution pH on CAP degradation by the EC/PMS system is shown in Fig. 6. The results showed that CAP degradation in the EC/PMS system was highly pH-dependent. As the initial pH increased from 3 to 11, the removal rate of CAP significantly decreased from 94.0 to 22.9%. The results showed that acidic conditions favored CAP degradation, and the optimum pH was 3 in this study, which is consistent with that of Fenton-like oxidation processes (Sheng et al. 1999). Because the speciation of Fe ions is highly dependent on the solution pH, as the pH increased from 3 to 11, the main forms of iron in the solution gradually changed from Fe^{2+} or Fe^{3+} to $Fe(OH)^+$, $FeOH^{2+}$, $Fe_2(OH)_2^{4+}$, and then finally transformed into $Fe(OH)_3$ (Eqs. (10)–(12)). This transformation resulted in the dramatic decrease in the percentage of free Fe^{2+}, leading to the reduction of $SO_4^{\bullet-}$ and slowing down CAP degradation (Lin et al. 2013). In addition, the reduction of iron ions in the cathode was also inhibited under alkaline conditions, which further delayed the degradation of CAP (Lakshmanan et al. 2009).

$$Fe^{2+} + H_2O \rightarrow Fe(OH)^+ + H^+ \quad (10)$$

$$Fe^{3+} + H_2O \rightarrow FeOH^{2+} + H^+ \quad (11)$$

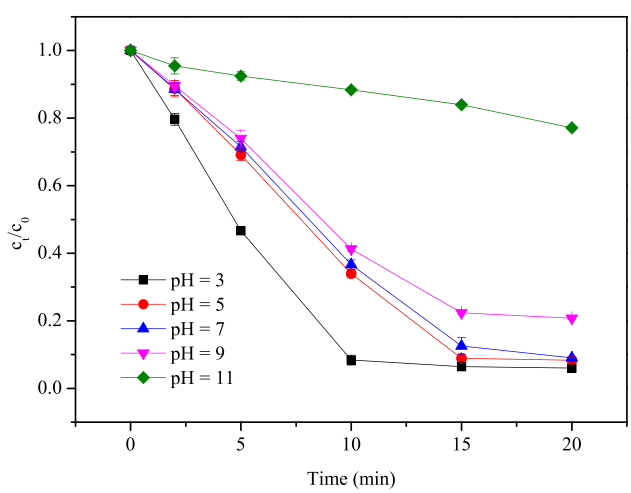

Fig. 6 Effect of initial pH on CAP degradation. Experimental conditions: $[CAP]_0$ = 10 μM, $[PMS]_0$ = 0.5 mM, current = 25 mA, $[Na_2SO_4]_0$ = 25 mM

$$2Fe^{3+} + 2H_2O \rightarrow Fe_2(OH)_2^{4+} + 2H^+ \quad (12)$$

Effect of common anions

Anions are ubiquitous in natural water and may affect $SO_4^{\bullet-}$-based oxidation process. Thus, it is necessary to explore the influence of these anions on the CAP degradation performance in the EC/PMS system. The effect of common anions, i.e., chloride (Cl^-), bicarbonate (HCO_3^-), and nitrate (NO_3^-), on CAP degradation by the EC/PMS system is shown in Fig. 7. Adding Cl^- only slightly enhanced the degradation of CAP, and the removal rate of CAP increased from 90.9 to 98.8% as the concentration of Cl^- increased from 0 to 10 mM. The addition of HCO_3^- or NO_3^- exerted a negative effect on CAP degradation performance, and the removal rates decreased from 90.9 to 26.6% and 66.3%, respectively, when the concentration of HCO_3^- or NO_3^- increased from 0 to 10 mM. The inhibition by HCO_3^- and NO_3^- could be ascribed to their scavenging effect on $SO_4^{\bullet-}$ and/or •OH as the following reactions (Eqs. (13)–(16)) (Ghauch and Tuqan 2012; Keen et al. 2012). However, in the presence of Cl^-, Cl^- reacted with $SO_4^{\bullet-}$ to form $Cl^{\bullet}$ (Eq. (17)), which then reacted with Cl^- to generate $Cl_2^{\bullet-}$ (Eq. (18)). The reactivities of $Cl^{\bullet}$ and $Cl_2^{\bullet-}$ with CAP may be similar to the reactivity between $SO_4^{\bullet-}$ and CAP (Lian et al. 2017). Furthermore, the transformation of $SO_4^{\bullet-}$ to reactive chlorine species can reduce the possibility of $SO_4^{\bullet-}$ scavenging by other $SO_4^{\bullet-}$ ions and/or PMS; this reduction in scavenging can compensate for the lower redox potential of $Cl^{\bullet}$ and $Cl_2^{\bullet-}$.

$$SO_4^{\bullet-} + HCO_3^- \rightarrow HSO_4^- + CO_3^{\bullet-} \quad (13)$$

$$\cdot OH + HCO_3^- \rightarrow H_2O + CO_3^{\bullet-} \quad (14)$$

$$SO_4^{\bullet-} + NO_3^- \rightarrow SO_4^{2-} + NO_3^{\bullet} \quad (15)$$

$$\cdot OH + NO_3^- \rightarrow OH^- + NO_3^{\bullet} \quad (16)$$

$$Cl^- + SO_4^{\bullet-} \rightarrow SO_4^{2-} + Cl^{\bullet} \quad (17)$$

$$Cl^{\bullet} + Cl^- \rightarrow Cl_2^{\bullet-} \quad (18)$$

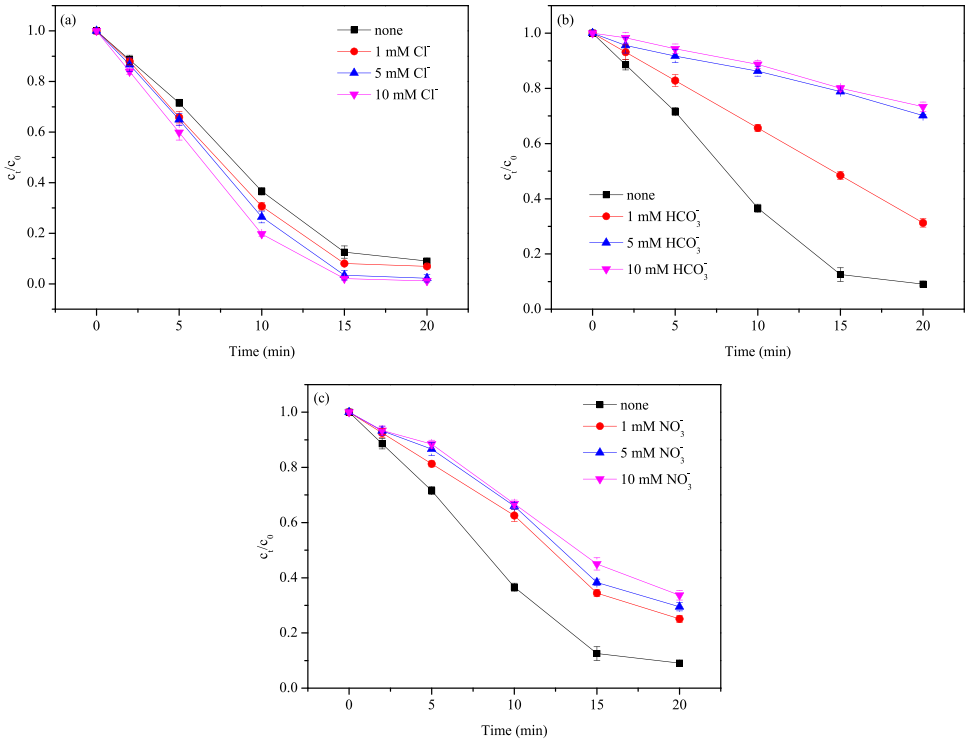

Fig. 7 Effect of different concentrations of **a** Cl^-, **b** HCO_3^-, and **c** NO_3^- on CAP degradation. Experimental conditions: $[CAP]_0 = 10\ \mu M$, $[PMS]_0 = 0.5$ mM, current = 25 mA, $[Na_2SO_4]_0 = 25$ mM, $pH_0 = 7$

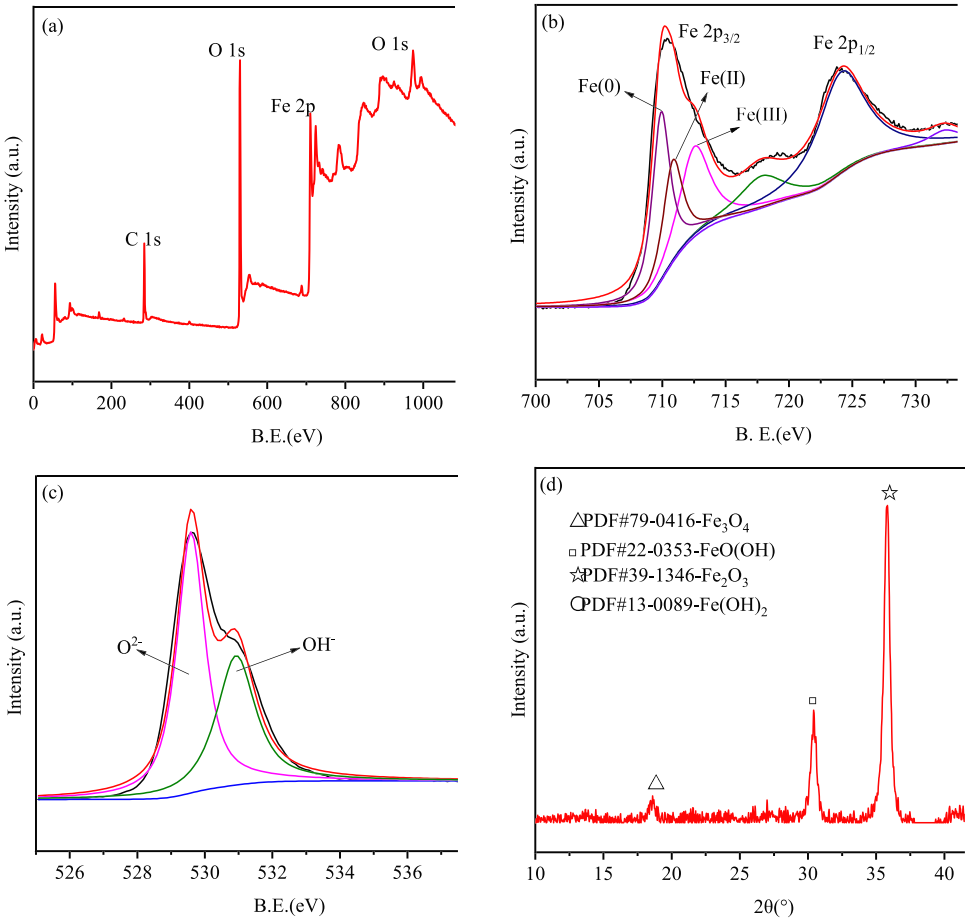

Fig. 8 **a** XPS full spectrum, **b** Fe 2p spectrum, **c** O 1s spectrum, and **d** XRD pattern of the floccules formed during the reaction

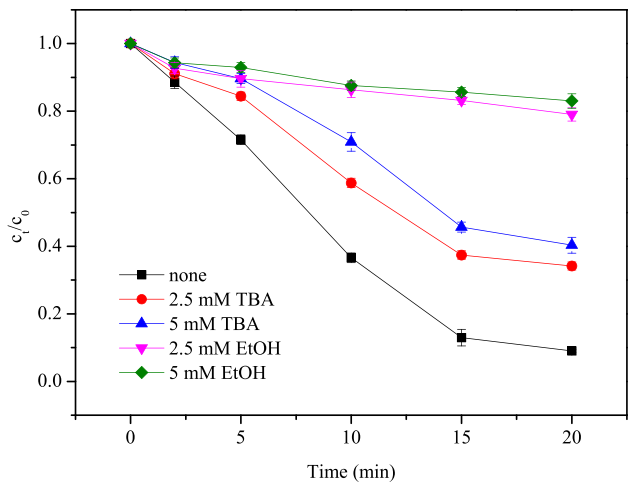

Fig. 9 Effect of radical scavengers on CAP degradation. Experimental conditions: $[CAP]_0$ = 10 μM, $[PMS]_0$ = 0.5 mM, current = 25 mA, $[Na_2SO_4]_0$ = 25 mM, pH_0 = 7

Degradation mechanism in the EC/PMS system

Characterization of floccules formed during the reaction

The composition of the floccules was analyzed after the reaction by XPS and XRD, and the results are shown in Fig. 8. According to the XPS full spectrum (Fig. 8a), the presence of Fe 2p, O 1s, and C 1s was observed in the floccules. The charge states of the elements in the formed floccules were determined by scanning the Fe 2p and O 1s orbitals. As shown in Fig. 8b, there are two spin-orbit separation peaks of the Fe $2p_{3/2}$ and Fe $2p_{1/2}$ core levels at binding energies of 710.4 eV and 723.9 eV, respectively (Xia et al. 2017). The peak positions of the Fe $2p_{3/2}$ level of Fe(III), Fe(II), and Fe(0) are at 712.6 eV, 710.9 eV, and 709.9 eV, respectively. The results indicate that Fe(III), Fe(II), and Fe(0) were present in the floccules after the reaction, and their main forms may be Fe_2O_3, Fe_3O_4, and FeO(OH) (Xu and Wang 2017). When flocculation occurs during electrolysis, the cathode reduces some of the Fe^{2+} to form Fe^0. The fine O 1s spectrum was also measured, as shown in Fig. 8c. Two intense peaks were observed at 529.6 eV and 530.9 eV. According to previous reports, O^{2-} is found near 529.7~530.1 eV, which confirms the presence of Fe_2O_3 and Fe_3O_4 in the floccules (Piumetti et al. 2015). The peak at 530.9 eV indicates the presence of hydroxides, such as FeO(OH), $Fe(OH)_2$, and $Fe(OH)_3$ (Al-Shamsi and Thomson 2013). According to both the XRD patterns (Fig. 8d) and XPS results of the floccules, the main components of the floccules are iron oxides (Fe_2O_3 and Fe_3O_4) and iron hydroxides (FeO(OH), $Fe(OH)_2$, and $Fe(OH)_3$). Therefore, in addition to coagulation and/or complexation caused by the formed floccules, PMS activation may occur, generating $SO_4^{\bullet-}$ and resulting in the promotion of CAP degradation. (He et al. 2016; Matzek and Carter 2016).

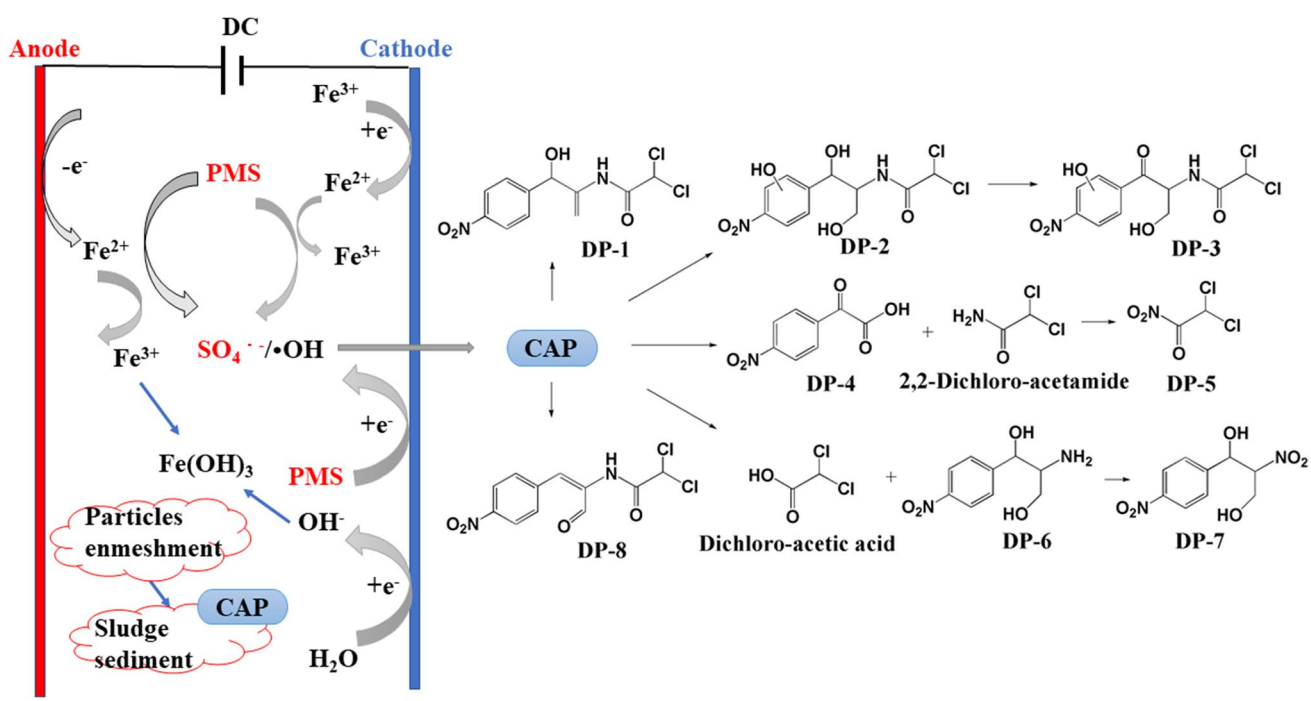

Fig. 10 Reaction mechanism and CAP degradation pathways during the EC/PMS process. Experimental conditions: $[CAP]_0$ = 10 μM, $[PMS]_0$ = 0.5 mM, current = 25 mA, $[Na_2SO_4]_0$ = 25 mM, pH_0 = 7

Table 1 Major DPs of CAP in the EC/PMS system identified by LC/TOF/MS

Compound	Retention time (RT) (min)	Experimental Mass $[M-H]^-$ (m/z)	Formula	Structure
CAP	5.373	323.1464	$C_{11}H_{12}N_2O_5Cl_2$	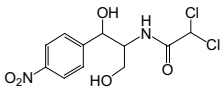
DP-1	5.255	305.0094	$C_{11}H_{10}Cl_2N_2O_4$	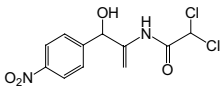
DP-2	8.112	338.3417	$C_{11}H_{11}N_2O_6Cl_2$	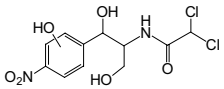
DP-3	10.451	335.2198	$C_{11}H_9N_2O_6Cl_2$	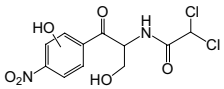
DP-4	9.496	195.1019	$C_8H_5NO_5$	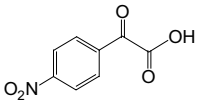
DP-5	6.483	158.1902	$C_2HCl_2NO_3$	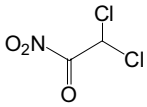
DP-6	9.750	211.1309	$C_9H_{12}N_2O_4$	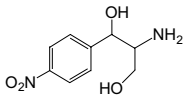
DP-7	9.929	241.1774	$C_9H_{10}N_2O_6$	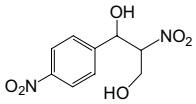
DP-8	10.933	301.1422	$C_{11}H_7N_2O_4Cl_2$	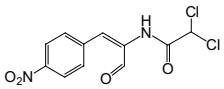

Reactive radical species identification

To verify the roles of the different reactive radical species in the EC/PMS system, quenching experiments were conducted in the presence of tert butanol (TBA) and ethanol (EtOH). EtOH (with α-hydrogen) is a well-known radical scavenger for both $SO_4^{\bullet-}$ and •OH because it can react quickly with both $SO_4^{\bullet-}$ and •OH with rate constants of $(1.6–7.7) \times 10^7$

and (1.2–2.8) × 10^9 M^{-1} s^{-1}, respectively, whereas TBA (without α-hydrogen) mainly quenches •OH because it can react more quickly with •OH ((3.8–7.6) × 10^8 M^{-1} s^{-1}) than with $SO_4^{\bullet-}$ ((4.0–9.1) × 10^5 M^{-1} s^{-1}) (Hu et al. 2020). Figure 9 shows the CAP removal efficiency in the presence of EtOH or TBA. The addition of EtOH significantly reduced the removal rate of CAP, and the removal efficiency of CAP decreased from 91.0 to 21.0% and 16.9% in the presence of 2.5 and 5 mM EtOH, respectively, after a reaction time of 20 min, suggesting that both $SO_4^{\bullet-}$ and •OH played an important role in CAP degradation. Moreover, the degradation of CAP was less inhibited by the presence of TBA, and the removal efficiency of TBA decreased from 91.0 to 65.8% and 58.6% in the presence of 2.5 and 5 mM TBA, indicating that compared to $SO_4^{\bullet-}$, •OH played a less important role in CAP degradation in the EC/PMS at neutral pH.

Degradation products and transformation pathways

According to the above results, the possible reaction mechanism for the EC/PMS system was proposed, as shown in Fig. 10. In the EC/PMS system, Fe^{2+} was slowly produced from the sacrificial iron anode through electrochemical corrosion and simultaneously released into the reaction solution (Eq. (1)), which could activate PMS in solution to generate $SO_4^{\bullet-}$ and/or •OH according to Eq. (2). The absorbed Fe^{3+} on the cathode can be reduced to Fe^{2+} via an electron transfer reaction according to Eq. (3), facilitating the Fe^{3+}/Fe^{2+} cycle, which reduces the wastage of the anode and maintains Fe^{2+} and radicals at appropriate concentrations (Li et al. 2018). Additionally, the adsorbed PMS on the cathode could also produce $SO_4^{\bullet-}$ and/or •OH (Eqs. (4) and (5)). The formed floccules, such as $Fe(OH)_3$, may also serve as coagulants, which can remove CAP through an enmeshment mechanism.

To further clarify the degradation mechanism, LC/TOF/MS was performed to identify the degradation products of CAP in the EC/PMS system. According to the results, in addition to CAP, eight major degradation products were found, and all these intermediates are summarized in Table 1. Based on the identified degradation products and previous studies, the degradation pathways of CAP were tentatively proposed in Fig. 10.

According to previous studies (Dong et al. 2017; Nie et al. 2018), DP-1 was identified as 2,2-dichloro-N-(1-(4-nitrobenzoyl)vinyl) acetamide, which is a dehydration product of CAP. During $SO_4^{\bullet-}$-induced oxidation, hydroxylation of the aromatic ring may occur by $SO_4^{\bullet-}$ attack through electron transfer or by •OH attack through hydroxyl addition; thus, DP-2 was identified as the hydroxylated product of CAP (Dulova et al. 2017). With further oxidation, the hydroxyl group in the side chain of partial CAP transformed into carbonyl groups to yield DP-3. Reactive radicals preferentially attacked the –C–N– bond in the side chain of partial CAP, leading to the formation of DP-4 and 2,2-dichloroacetamide, followed by further oxidation of 2,2-dichloroacetamide to yield DP-5 (Nie et al. 2018). Under the attack of •OH, CAP was broken down into dichloro-acetic acid and DP-6. The amino group of DP-6 was further oxidized to the nitro group of DP-7 (Garcia-Segura et al. 2014). The formation of DP-8 indicated that both dehydration and the transformation of hydroxyl groups to aldehyde groups might occur at CAP. Then, these intermediate products were further degraded to smaller molecule compounds and finally mineralized to H_2O and CO_2.

Conclusion

This study showed that an electrochemically activated peroxymonosulfate (EC/PMS) system can effectively remove CAP from water, and the removal efficiency is better than that of EC alone, PMS alone, and the Fe^{2+}/PMS system. Increasing the applied current and electrolyte concentration enhanced CAP degradation, and the optimal PMS dose for the removal of CAP was 0.5 mM. The removal of CAP is highly pH-dependent, and acidic conditions facilitate CAP degradation. The presence of Cl^- slightly promoted CAP degradation, whereas HCO_3^- and NO_3^- exhibited inhibitory effects on CAP degradation. The main components of the floccules after the reaction included iron oxides (i.e., Fe_2O_3 and Fe_3O_4) and iron hydroxides (i.e., FeO(OH) and $Fe(OH)_3$), as reflected by the XPS and XRD analysis results. The results of quenching experiments indicated that both $SO_4^{\bullet-}$ and •OH were responsible for the degradation of CAP. CAP degradation products were identified by LC/TOF/MS, and the primary degradation pathway was proposed.

Author contribution Yu-Qiong Gao: conceptualization, methodology, funding acquisition, writing—review and editing
Jin-Qiang Zhou: investigation, visualization, writing—original draft
Han Ning: investigation, validation
Yan-Yan Rao: formal analysis, validation
Nai-Yun Gao: supervision

Funding This work was funded by the National Natural Science Foundation of China (51708348); the Scientific and Innovative Action Plan of Shanghai, China (19DZ1208204); and State Key Laboratory of Pollution Control and Resource Reuse Foundation (PCRRF18005).

Data availability All data generated or analyzed during this study are included in this published article.

Declarations

Ethics approval Not applicable

Consent to participate Not applicable

Consent for publication Not applicable

Competing interests The authors declare no competing interests.

References

Ali J, Wenli L, Shahzad A, Ifthikar J, Aregay GG, Shahib II, Elkhlifi Z, Chen ZL, Chen ZQ (2020) Regulating the redox centers of Fe through the enrichment of Mo moiety for persulfate activation: a new strategy to achieve maximum persulfate utilization efficiency. Water Res 181:115862

Al-Shamsi MA, Thomson NR (2013) Treatment of organic compounds by activated persulfate using nanoscale zerovalent iron. Ind Eng Chem Res 52:13564–13571

Brillas E, Sirés I, Oturan MA (2009) Electro-Fenton process and related electrochemical technologies based on Fenton's reaction chemistry. Chem Rev 109:6570–6631

Cao Y, Qiu W, Zhao YM, Li J, Jiang J, Yang Y, Pang SY, Liu GQ (2020) The degradation of chloramphenicol by O_3/PMS and the impact of O_3-based AOPs pre-oxidation on dichloroacetamide generation in post-chlorination. Chem Eng J 401:126146

Danner M-C, Robertson A, Behrends V, Reiss J (2019) Antibiotic pollution in surface fresh waters: occurrence and effects. Sci Total Environ 664:793–804

Dong HY, Qiang ZM, Hu J, Qu JH (2017) Degradation of chloramphenicol by UV/chlorine treatment: kinetics, mechanism and enhanced formation of halonitromethanes. Water Res 121:178–185

Dulova N, Kattel E, Trapido M (2017) Degradation of naproxen by ferrous ion-activated hydrogen peroxide, persulfate and combined hydrogen peroxide/persulfate processes: The effect of citric acid addition. Chem Eng J 318:254–263

Fan Y, Wang B, Yuan S, Wu X, Chen J, Wang L (2010) Adsorptive removal of chloramphenicol from wastewater by NaOH modified bamboo charcoal. Bioresour Technol 101:7661–7664

Garcia-Segura S, Cavalcanti EB, Brillas E (2014) Mineralization of the antibiotic chloramphenicol by solar photoelectro-Fenton: from stirred tank reactor to solar pre-pilot plant. Appl Catal B Environ 144:588–598

Ghauch A, Tuqan AM (2012) Oxidation of bisoprolol in heated persulfate/H_2O systems: Kinetics and products. Chem Eng J 183:162–171

Govindan K, Raja M, Noel M, James EJ (2014) Degradation of pentachlorophenol by hydroxyl radicals and sulfate radicals using electrochemical activation of peroxomonosulfate, peroxodisulfate and hydrogen peroxide. J Hazard Mater 272:42–51

He J, Yang XF, Men B, Wang DS (2016) Interfacial mechanisms of heterogeneous Fenton reactions catalyzed by iron-based materials: a review. J Environ Sci 39:97–109

Hirsch R, Ternes T, Haberer K, Kratz KL (1999) Occurrence of antibiotics in the aquatic environment. Sci Total Environ 225:109–118

Hu CY, Hou YZ, Lin YL, Deng YG, Hua SJ, Du YF, Chen CW, Wu CH (2020) Investigation of iohexol degradation kinetics by using heat-activated persulfate. Chem Eng J 379:122403

Huang WX, Fu BM, Fang SY, Wang F, Shao QQ, Du W, Fang F, Feng Q, Cao JS, Luo JY (2021) Insights into the accelerated venlafaxine degradation by cysteine-assisted Fe^{2+}/persulfate: key influencing factors, mechanisms and transformation pathways with DFT study. Sci Total Environ 793:148555

Keen OS, Love NG, Linden KG (2012) The role of effluent nitrate in trace organic chemical oxidation during UV disinfection. Water Res 46:5224–5234

Kovalakova P, Cizmas L, McDonald TJ, Marsalek B, Feng MB, Sharma VK (2020) Occurrence and toxicity of antibiotics in the aquatic environment: a review. Chemosphere 251:126351

Kümmerer K (2009) Antibiotics in the aquatic environment - a review - Part I. Chemosphere 75:417–434

Lakshmanan D, Clifford DA, Samanta G (2009) Ferrous and ferric ion generation during iron electrocoagulation. Environ Sci Technol 43:3853–3859

Lian LS, Yao B, Hou SD, Fang JY, Yan SW, Song WH (2017) Kinetic study of hydroxyl and sulfate radical-mediated oxidation of pharmaceuticals in wastewater effluents. Environ Sci Technol 51:2954–2962

Lin H, Wu J, Zhang H (2013) Degradation of bisphenol A in aqueous solution by a novel electro/Fe^{3+}/peroxydisulfate process. Sep Purif Technol 117:18–23

Li J, Ren Y, Lai LD, Lai B (2018) Electrolysis assisted persulfate with annular iron sheet as anode for the enhanced degradation of 2,4-dinitrophenol in aqueous solution. J Hazard Mater 344:778–787

Matzek LW, Carter KE (2016) Activated persulfate for organic chemical degradation: a review. Chemosphere 151:178–188

Nie MH, Yan CX, Xiong XY, Wen XM, Yang X, Lv ZL, Dong WB (2018) Degradation of chloramphenicol using a combination system of simulated solar light, Fe^{2+} and persulfate. Chem Eng J 348:455–463

Oh WD, Dong ZL, Lim TT (2016) Generation of sulfate radical through heterogeneous catalysis for organic contaminants removal: current development, challenges and prospects. Appl Catal B Environ 194:169–201

Periyasamy S, Muthuchamy M (2018) Electrochemical oxidation of paracetamol in water by graphite anode: effect of pH, electrolyte concentration and current density. J Environ Chem Eng 6:7358–7367

Piumetti M, Fino D, Russo N (2015) Mesoporous manganese oxides prepared by solution combustion synthesis as catalysts for the total oxidation of VOCs. Appl Catal B Environ 163:277–287

Qi CD, Liu XT, Li Y, Lin CY, Ma J, Li XW, Zhang HJ (2017) Enhanced degradation of organic contaminants in water by peroxydisulfate coupled with bisulfite. J Hazard Mater 328:98–107

Rastogi A, Al-Abed SR, Dionysiou DD (2009) Sulfate radical-based ferrous-peroxymonosulfate oxidative system for PCBs degradation in aqueous and sediment systems. Appl Catal B Environ 85:171–179

Sheng HL, Chi ML, Leu HG (1999) Operating characteristics and kinetic studies of surfactant wastewater treatment by Fenton oxidation. Water Res 33:1735–1741

Shukla P, Fatimah I, Wang SB, Ang HM, Tadé MO (2010) Photocatalytic generation of sulphate and hydroxyl radicals using zinc oxide under low-power UV to oxidise phenolic contaminants in wastewater. Catal Today 157:410–414

Song HR, Yan LX, Wang YW, Jiang J, Ma J, Li CP, Wang G, Gu J, Liu P (2020) Electrochemically activated PMS and PDS: radical oxidation versus nonradical oxidation. Chem Eng J 391:123560

Tan CQ, Dong YJ, Shi L, Chen Q, Yang SW, Liu XY, Ling JF, He XF, Fu DF (2018) Degradation of Orange II in ferrous activated peroxymonosulfate system: efficiency, situ EPR spin trapping and degradation pathway study. J Taiwan Inst Chem E 83:74–81

Wacławek S, Grübel K, Černík M (2015) Simple spectrophotometric determination of monopersulfate. Spectrochim Acta Part A 149:928–933

Wang YR, Chu W (2011) Degradation of 2,4,5-trichlorophenoxyacetic acid by a novel electro-Fe(II)/oxone process using iron sheet as the sacrificial anode. Water Res 45:3883–3889

Wang YR, Chu W (2012) Photo-assisted degradation of 2,4,5-trichlorophenoxyacetic acid by Fe(II)-catalyzed activation of oxone process: the role of UV irradiation, reaction mechanism and mineralization. Appl Catal B Environ 123-124:151–161

Wu D, Sun FQ, Zhou Y (2017) Degradation of chloramphenicol with novel metal foam electrodes in bioelectrochemical systems. Electrochim Acta 240:136–145

Xia XF, Ling L, Zhang WX (2017) Solution and surface chemistry of the Se(IV)-Fe(0) reactions: effect of initial solution pH. Chemosphere 168:1597–1603

Xu L, Wang J (2017) Magnetic nanoscaled Fe_3O_4/CeO_2 composite as an efficient Fenton-like heterogeneous catalyst for degradation of 4-chlorophenol. Environ Sci Technol 46:10145–10153

Xu WH, Zhang G, Zou SC, Li XD, Liu YC (2007) Determination of selected antibiotics in the Victoria Harbour and the Pearl River, South China using high-performance liquid chromatography-electrospray ionization tandem mass spectrometry. Environ Pollut 145:672–679

Yan CX, Yang Y, Zhou JL, Nie MH, Liu M, Hochella MF Jr (2015) Selected emerging organic contaminants in the Yangtze Estuary, China: a comprehensive treatment of their association with aquatic colloids. J Hazard Mater 283:14–23

Zhang Z, Li X, Zhang C, Lu S, Xi Y, Huang Y, Xue Z, Yang T (2021) Combining ferrate(VI) with thiosulfate to oxidize chloramphenicol: influencing factors and degradation mechanism. J Environ Chem Eng 9:104625

Zhou JH, Chen KB, Hong QK, Zeng FC, Wang HY (2017) Degradation of chloramphenicol by potassium ferrate(VI) oxidation: kinetics and products. Environ Sci Pollut Res 24:10166–10171

Zhou JL, Zhang ZL, Banks E, Grover D, Jiang JQ (2009) Pharmaceutical residues in wastewater treatment works effluents and their impact on receiving river water. J Hazard Mater 166:655–661

Zou J, Ma J, Chen LW, Li XC, Guan YH, Xie PC, Pan C (2013) Rapid acceleration of ferrous iron/peroxymonosulfate oxidation of organic pollutants by promoting Fe(III)/Fe(II) cycle with hydroxylamine. Environ Sci Technol 47:11685–11691